ACS APPLIED MATERIALS & INTERFACES

Research Article

www.acsami.org

Mesoporous Silica Nanoparticles Capped with Disulfide-Linked PEG Gatekeepers for Glutathione-Mediated Controlled Release

Yanna Cui,[†] Haiqing Dong,[‡] Xiaojun Cai,[‡] Deping Wang,*[,†] and Yongyong Li*[,‡]

[†]School of Material Science and Engineering, Tongji University, Shanghai, 201804, P. R. China

[‡]The Institute for Advanced Materials and Nano Biomedicine, School of Medicine, Tongji University, Shanghai, 200092, P. R. China

ABSTRACT: Hybrid mesoporous silica nanoparticles (MSNs), which were synthesized using the co-condensation method and engineered with unique redox-responsive gatekeepers, were developed for studying the glutathione-mediated controlled release. These hybrid nanoparticles constitute a mesoporous silica core that can accommodate the guests (i.e., drug, dye) and the PEG shell that can be connected with the core via disulfide-linker. Interestingly, the PEG shell can be selectively detached from the inner core at tumor-relevant glutathione (GSH) levels and facilitate the release of the encapsulated guests at a controlled manner. The structure of the resulting hybrid nanoparticles (MSNs-SS-mPEG) was comprehensively characterized by transmission electron microscopy (TEM), Fourier transform infrared spectroscopy (FTIR), powder X-ray diffraction (XRD), and nitrogen adsorption/desorption isotherms analysis. The disulfide-linked PEG chains anchored on MSNs could serve as efficient gatekeepers to control the on−off of the pores. Compared with no GSH, fluorescein dye as the model drug loaded into MSNs showed rapid release in 10 mM GSH, indicating the accelerated release after the opening of the pores regulated by GSH. Confocal microscopy images showed a clear evidence of the dye-loaded MSNs-SS-mPEG nanoparticles endocytosis into MCF-7 cells and releasing guest molecules from the pore inside cells. Moreover, in vitro cell viability test using MTT assay indicated that MSNs-SS-mPEG nanoparticles had no obvious cytotoxicity. These results indicate that MSNs-SS-mPEG nanoparticles can be used in the biomedical field.

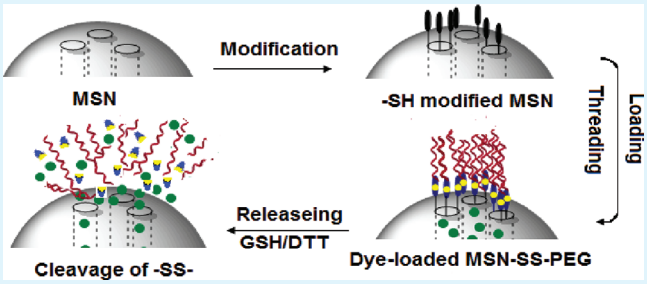

KEYWORDS: *mesoporous silica nanoparticles (MSNs), MSNs-SS-PEG nanoparticles, reduction-sensitive, PEG gatekeeper, controlled release, cytotoxicity*

1. INTRODUCTION

Recently, mesoporous silica nanoparticles (MSNs) have been proven that they are extremely effective solid drug nanocontainers, due to their highly ordered mesopores, high surface areas, easily functionalized surface, large pore volume, and biocompatibility. In particular, mesoporous silica nanoparticles coated with stimuli-responsive gatekeepers can provide benefits from many aspects including transportation of guest molecules (i.e., drugs or dyes) to specific locations in the body, controlled release in response to either external triggering signals or cellular stimuli, such as pH,[1] temperature,[2] enzymes,[3] light,[4] redox agents,[5] and so on. The controlled release behavior is generally regulated by the on−off of the pore via its gatekeeper.

To date, various MSNs-based systems have been reported for the controlled-release of guests from the mesopores regulated by different mechanism. For example, MSNs-based systems capped with size-defined CdS[6] and Fe_3O_4[7] nanoparticles have been developed for redox-responsive controlled release. Acid-decomposable ZnO quantum dots[8] as the gatekeepers have been employed to inhibit premature drug release when they encounter the more acidic condition in tumors. Positively charged Au nanoparticles[9] have been utilized to block the nanopores of MSNs via electrostatic interaction controlled by UV irradiation. The pH-responsive poly (2-(diethylamino)ethyl methacrylate) (PDEAEMA)-coated MSNs[10] were prepared with the PDEAEMA brushes as a switch to control the opening and closing of the pores by adjusting the pH value of the solution. Among them, redox-responsive MSN-based nanosystems that can release drugs or dyes in response to an intracellular signal represent great superiority over their conventional counterparts. Glutathione (GSH) is the mostly used intracellular signal. Its concentration between the exterior (2 μM) and interior (10 mM) of the cells is significantly different.[11−13] Moreover, the cytosolic GSH level in some tumor cells has been found to be at least 4-fold higher compared with normal cells. Thus those nanosystems that can be responsive to GSH are expected to enable the intracellular drug release and specific to tumor cells. Recently, a few studies on the glutathione-mediated controlled release on MSNs nanosystems were reported. For example, Lin and co-workers[14] reported a MSN-based controlled intracellular cysteine release system, in which cysteine (Cys) was tethered to MSN via disulfide bonds (MSNs-SS-Cys). Park and Kim[5] demonstrated that tethering the CD gatekeepers via disulfide linker on the

Received: March 24, 2012
Accepted: May 30, 2012
Published: May 30, 2012

   dx.doi.org/10.1021/am3005225 | *ACS Appl. Mater. Interfaces* 2012, 4, 3177−3183

surface of Si-MPs is an efficient approach to entrap and release the guest by the switch of gatekeeper in response to GSH.

Herein, for the first time, MSNs-SS-mPEG nanosystem composed of the detachable PEG shell in response to GSH has been developed for controlled guest release, where the PEG shell and MSNs were connected via disulfide bond which is prone to be cleaved upon GSH. The PEG shell[15] was chosen for the reasons including: (i) PEG fictionalization has been known to prolong the circulation time and improve the enhanced permeability and retention (ERP) effect; (ii) PEG is biocompatible and its molecular size can be sufficient to cap the mesopores of MSN according to its molecular weight; (iii) PEG is attached to the nanoparticles to provide a "stealth" shielding effect, delaying the action of the reticuloendothelial system (RES).[16] Therefore, the purposes of the PEG chosen are expected to afford the MSNs with both physiological stability and capability of intracellular release.

In this research, we describe a novel PEG surface-capped mesoporous silica based nanosystem (MSNs-SS-mPEG) that can exhibits redox-responsive release characteristics and contains disulfide linkage. The MSNs-SS-mPEG nanoparticle consists of the mesoporous silica as a reservoir for guest molecules, a disulfide bond as a redox-responsive cleavable linker, and PEG "gatekeeper" that can close or open the gate of the pore of mesoporous silica. The proof-of-concept of the new design was supported by the controlled release of fluorescein dye, in vitro cytotoxicity against breast cancer cells (MCF-7) and cell uptake of these nanoparticles.

2. EXPERIMENTAL SECTION

2.1. Materials and Equipment. 3-Mercaptopropyltrimethoxysilane (MPTES), cetyltrimethyl-ammonium bromide (CTAB), tetraethylorthosilicate (TEOS), sodium hydroxide (NaOH), N, N-Dimethylformamide (DMF), polyethylene glycol orthopyridyl disulfide (mPEG-SS-Pyridine), 5(6)-Carboxyfluorescein, methotrexate (MTX), hydrochloric acid (HCl), and glutathione (GSH, 98%) were purchased from the Aladdin Chemistry, Co. (Shanghai) and used as received. Dulbecco's modified Eagle's medium (DMEM), fetal bovine serum (FBS), penicillin-streptomycin, trypsin were obtained from Gibco Invitrogen Corp. paraformaldehyde (4%) was purchased from DingGuo Chang Sheng Biotech. Co., Ltd.

Transmission electron microscopy (TEM) images of nanoparticles were carried out on a Hitachi H7100 transmission electron microscope (Hitachi, Ltd., Hong Kong) at an acceleration voltage of 100 kV. X-ray diffraction (XRD) patterns of the samples were collected using an X-ray diffractometer. Data were obtained from 1 to 10° (diffraction angle 2θ) at a step size of 0.006° and a scanning speed of 0.4°/min radiation. The pore structure was measured at 77 K on a Quantachrome instrument. Size distribution and Zeta potential of nanoparticles were determined using a Nano-ZS 90 Nanosizer (Malvern Instruments Ltd., Worcestershire, UK). FTIR spectra of powdered samples were recorded on a Tensor 27 FT-IR spectrometer (Bruker AXS, China). The cellular uptake was observed using a laser scanning confocal microscope (Leica TCS SP5 II, Germany) equipment at an excitation wavelength of 492 nm.

2.2. Preparation of Mesoporous Silica Nanoparticles (MSNs). MSNs were prepared by the modified Hyehyeon Kim's method to totally remove the surfactant.[5] An aqueous solution of cetyltrimethylammonium bromide (CTAB, 0.1 g) was added into the sodium hydroxide solution (2 M, 0.35 mL). After stirring at room temperature for 20 min, tetraethylorthosilicate (TEOS, 0.5 mL) was added to the solution. The reaction mixture was vigorously stirred at 80 °C for 2 h. After being filtered, washed thoroughly with methanol, and dried under a vacuum at 30 °C for 20 h, the resulting production was calcinated at 550 °C for 6 h to remove the redundant CTAB template.

2.3. Synthesis of MSNs-SH Nanoparticles. MSNs (90 mg) was dissolved in methanol (20 mL) and functionalized with 1.8 mL of 3-mercaptopropyltrimethoxysilane. The mixture was stirred at 50 °C for 24 h under nitrogen atmosphere. Then, the particles were separated by centrifugation (10 krpm, 20 min) and washed three times with methanol following the reported procedure.[5]

2.4. Synthesis of MSNs-SS-mPEG Nanoparticles. MSNs-SH (30 mg) was dissolved in anhydrous DMF (20 mL). mPEG-SS-Pyridine (40 mg) was added in the above solution, stirred at 50 °C for 24 h under nitrogen atmosphere, separated by centrifugation (10 krpm, 20 min), and washed several times with methanol and water.

2.5. Dye Loading and the Controlled Release. Fluorescein dye as a model drug (8 mg) was dissolved in 15 mL of PBS. Then MSNs-SH (30 mg) was added in the solution which was sonicated for 30 min, and stirred for about 24 h at 40 °C. The precipitate was centrifuged, washed extensively with PBS to remove the redundant dye on the surface of MSNs-SH. Subsequently, mPEG-SS-pyridine (36 mg) was dissolved in DCM solution (10 mL) with pH value adjusted to 2−3 by hydrochloric. MSNs-SH (30 mg) was added. The reaction was allowed to proceed for 24 h at 50 °C under nitrogen atmosphere to minimize the air oxidation. The resulting MSNs-SS-mPEG nanoparticles were isolated by precipitation in methanol and purified by washing with methanol/water for 3 times. The excessive mPEG-SS-pyridine was removed during precipitation in methanol. To investigate the redox-responsive release, the control experiments were carried out by dissolving dye-loaded MSNs-SS-mPEG (3 mg) into PBS with different concentration of GSH, shaking at 150 rpm (37 °C). At specified time intervals, 3 mL of PBS was taken out in order to test the released fluorescein dye and replenished with an equal volume of fresh PBS.

Dye loading efficiency (LE) in MSNs-SH was quantified by UV−vis spectroscopy. LE of dye in MSNs-SH is expressed as % of total dye added according to

$$\mathrm{LE}[\%] = \left(\frac{\text{mass of dye in MSNs-SH}}{\text{mass of total dye added}}\right) \times 100\% \quad (1)$$

The cumulative amount of dye released from the MSNs-SS-mPEG over 22 h was calculated according to

$$\text{cumulative dye release } (\%) = \left(\frac{M_t}{M_0}\right) \times 100\% \quad (2)$$

Where M_t is the total amount of dye released from MSNs-SS-mPEG at time t, and M_0 is the amount of dye initially loaded into the MSNs-SS-mPEG.

2.6. In vitro Cell Proliferation Assay. For experiments, Human MCF-7 breast cancer cells were routinely incubated at 37 °C in a humidified 5% CO_2 atmosphere using DMEM supplemented with 10% fetal bovine serum and 0.1% penicillin-streptomycin. MCF-7 cells were seeded into 96-well plate at a density of 5×10^3 cells/well. After 24 h, cells were then exposed for another 24 h to various MSNs-SS-mPEG nanoparticles with concentration of ranging from 0.125 to 1 mg/mL that were prepared in cell culture media. At the end of the incubation period, the volume in each well was replaced with 200 μL of fresh media and 20 μL of 5 mg/mL sterile filtered 3-(4,5)-dimethylthiahiazo(-z-y1)-3,5-diphenytetrazoliumromide (MTT)[17] solution in PBS. The plate was incubated for additional 4 h at 37 °C, allowing viable cells to metabolically reduce MTT into purple formazan. After addition of 150 μL of dimethyl sulfoxide (DMSO) to each well, the plate was incubated at RT for 10 min on a shaking platform before optical density (OD) was measured at λ= 492 nm using a Multiscan MK3 plate reader (Thermo Fisher Scientific, Waltham, MA, USA). Relative cell viability in % was calculated according to

$$\text{cell viability} = \left(\frac{\mathrm{OD}_{\text{treated}} - \mathrm{OD}_{\text{blank}}}{\mathrm{OD}_{\text{controlled}} - \mathrm{OD}_{\text{blank}}}\right) \times 100\% \quad (3)$$

Scheme 1. (a) Illustration of (a) Synthesis of the Dye-Loaded MSNs-SS-mPEG Nanoparticles and the Mechanism of Dye Release by Disulfide Cleavage; (b) Exchange Reaction between MSNs-SH and PEG-SS-Pyridine

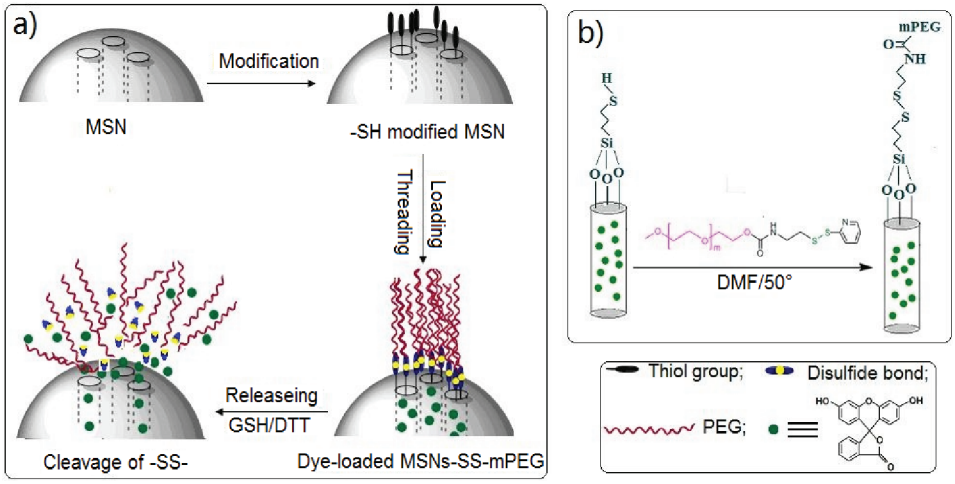

Where $OD_{treated}$ is obtained by comparing the OD with control wells containing only cell culture medium, OD_{blank} contains only the DMEM.

2.7. Cell Uptake. MCF-7 cells were incubated in a 6-well plate at a density of 1×10^5 cells/well for 24 h in a humidified atmosphere with 5% CO_2 at 37 °C. Then, the cells were washed by PBS and incubated at 37 °C for another 24 h with dye-loaded MSNs-SS-mPEG nanoparticles in complete medium. The cells were washed with PBS twice and fixed with paraformaldehyde (4%). Next, they are immersed in DAPI (4′, 6-diamidino-2- phenylindole) for about 10 min. Finally, the slides were mounted and observed under a laser scanning confocal microscope (Olympus, FV300, IX71, Tokyo, Japan) equipment.

3. RESULTS AND DISCUSSION

3.1. Synthesis and Characterization. The synthesis process of the mesoporous silica-based nanoparticles with PEG gatekeepers connected via disulfide linker was summarized in Scheme 1. Mesoporous silica nanoparticles (MSNs) were synthesized according to the previous method.[5] The resulting MSNs were insoluble in the aqueous media. In this study, disulfide-linked PEG was employed to coat MSNs to confer them with high physiological stability. However, PEG was found to be a significant diffusion barrier impeding the release of the loaded drug. To resolve this issue as well as establish a triggering release mechanism, we engineered PEG-coated MSNs hybrid nanoparticles by conjugating PEG to thiol-functionalized MSNs via a disulfide bond. In the last chemical procedure, MSNs-SS-mPEG was synthesized by exchange reaction between the thiol end group functionalized mesoporous silica nanoparticles (MSNs-SH) and the pyridyldisulfide groups at the end of PEG (i.e., mPEG-SS-pyridine). This unique system of MSNs-SS-mPEG will not only present great advantage on the high stability in physiological solution, but also can facilitate the release of the encapsulated guest molecules triggered by tumor-relevant GSH level.

The structures of MSNs and MSNs-SS-mPEG nanoparticles were carried out and monitored by transmission electron microscopy (TEM), X-ray diffraction (XRD), N_2 adsorption/desorption isotherm, and dynamic light scattering (DLS). Figure 1 showed TEM images of MSNs and MSNs-SS-mPEG nanoparticles, where Figure 1a illustrated the representative TEM image of MSNs prepared in the water solution with a CTAB concentration at 5.716 mM. The resulting MSNs showed an average diameter of about 70 nm and retained their

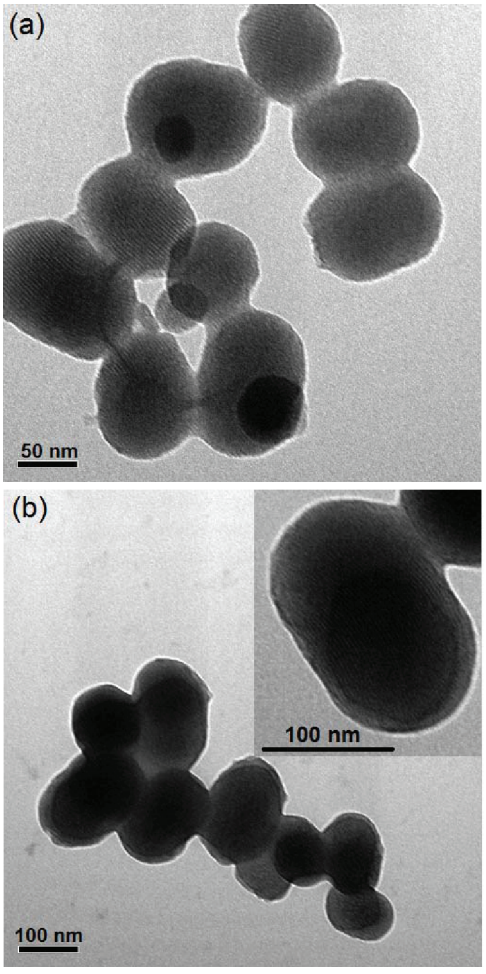

Figure 1. TEM images of (a) MSNs and (b) MSN-SS-mPEG nanoparticles.

intact ordered mesoporous property even after being calcined at 550 °C for 6 h. In Figure 1b, the enlargement in the upper right distinctively appeared the PEG nanoshell surrounding the core of MSNs, which could be identified by noticeable contrast between the core and the shell of the MSNs-SS-mPEG nanoparticles. The particle size of MSNs-SS-mPEG was 100–

dx.doi.org/10.1021/am3005225 | ACS Appl. Mater. Interfaces 2012, 4, 3177–3183

150 nm. The thickness of PEG shell was 10−30 nm and could be controlled by adjusting the amount of the mPEG-SS-Pyridine. Meanwhile, the parallel strips in the core area indicated that the polymerization of PEG did not destroy the mesoporous trait of MSNs.

Particle size and their distributions of the samples in H_2O were measured by dynamic light scattering (DLS) as shown in Figure 2. Compared with the TEM data, the overall size of

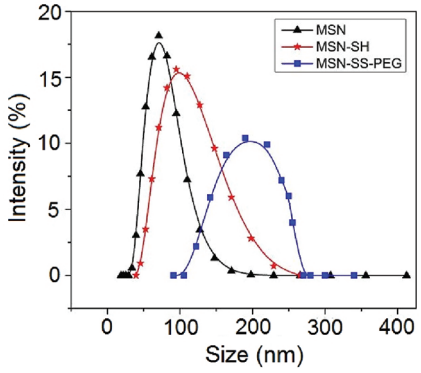

Figure 2. Size distributions of MSNs, MSN-SH, and MSN-SS-mPEG determined by DLS.

MSNs-SS-mPEG size measured by DLS was slightly larger than that of TEM results. Different principles between these two characterizations are believed to be the main reason for this phenomenon. Generally, DLS gives the hydrodynamic size of nanoparticles whereas TEM results in the size of nanoparticles in a dried state. In this study, the hydrodynamic radius of MSNs-SS-mPEG nanoparticles measured by DLS corresponds to the radius of the dense core, plus the thickness of the hydration layer arising from the very hydrophilic PEG in nanoparticles surface. In contrast, TEM only provides the size of the nanoparticle in a dried state without hydration layer. Similar results have been observed in other works.[15,18,19] From the DLS data, it was further observed that MSNs-SS-mPEG nanoparticles showed a larger hydrodynamic diameter (D_h) than that of MSNs, ascribed to the surface cap of PEG induced by chain−chain repulsions and chain-solvent interactions, thus resulting in a larger D_h. Besides, zeta potential of MSNs, MSN-SH, and MSNs-SS-mPEG was −36.4 eV, −43.3 eV, and −27.8 eV, respectively, indicating an anionic surface of the nano-system which was reported to optimal for more compatibility with blood compared with their cationic counterparts.[20]

The TGA curve of MSNs-SS-mPEG nanoparticles was shown in Figure 3. It can be seen that MSNs-SS-mPEG nanoparticles yielded about 9.2% weight loss from ca. 25 to 280 °C, which attributed to the desorption of physically adsorbed water. An additional weight loss occurred between 280 and 400 °C due to the further condensation of the silica mesoporous walls. The decline in the temperature range from ca. 400 to 800 °C should be ascribed to the removal of polymer on the surface when heating in the nitrogen atmosphere.

The powder X-ray diffraction (XRD) (Figure 4) was applied to characterize the structures of MSNs and MSNs-SS-mPEG nanoparticles. XRD pattern of MSNs (Figure 4) exhibited a much stronger diffraction peak in the low 2θ region, about 2.2°, typical of short-range ordered mesoporous phase. XRD pattern of MSNs-SS-mPEG (Figure 4(b)) also exhibited a very

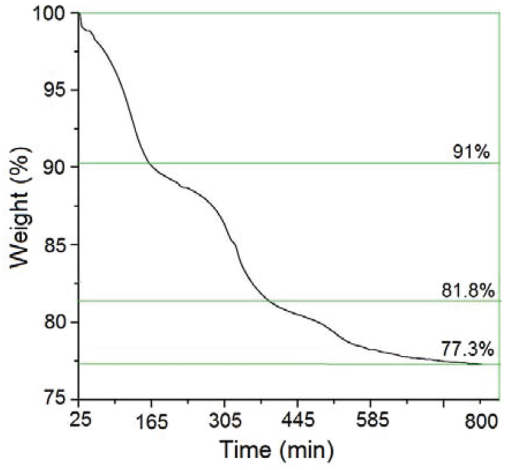

Figure 3. TGA curve of MSNs-SS-mPEG nanoparticle.

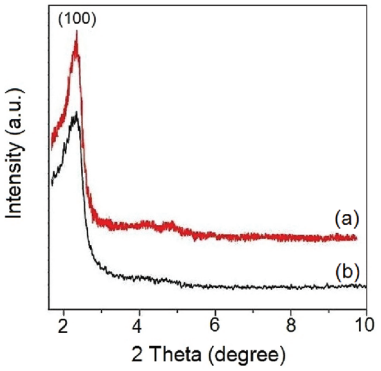

Figure 4. XRD patterns of (a) MSNs, (b) MSNs-SS-mPEG.

stronger diffraction peak in the low 2θ region, suggesting the high structural stability after the conjugation of the PEG chains.

FTIR spectra for the MSNs, the MSNs-SH, and the resulting MSNs-SS-mPEG are all shown in Figure 5. The vibrational

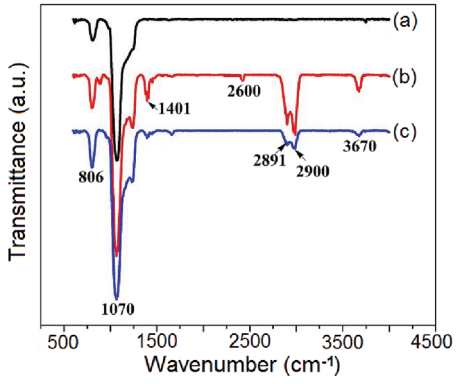

Figure 5. FTIR spectra of (a) MSNs, (b) MSNs-SH, (c) MSNs-SS-mPEG nanoparticles.

peak can be clearly observed at 2600 cm^{-1}, which was assigned to the thiol group. Vibrational peaks at 2930, 2891, and 1401 cm^{-1} were assigned to symmetric stretching and bending of C−H groups due to the addition of PEG chains by exchange reaction between the mercaptopropyl group of MSNs-SH and disulfide group of PEG orthopyridyl disulfide (mPEG-SS-Pyridine). The Si−OH band at 1070 cm^{-1} and 806 cm^{-1}

became significantly weaker after the thiol group or PEG chain modification. These results suggested that thiol group and PEG chains had been grafted onto the surface of MSNs.

The nitrogen adsorption and desorption isotherm at 77 K for the calcined MSNs sample showed the type isotherm characteristics with the value of P/P_0 range from 0.85 to 0.95. The relatively high value of their specific surface area calculated from the linear part of the Brunauer–Emmett–Teller (BET) plot reached 766 m^2 g^{-1} with the pore volume of 0.66 m^3 g^{-1}, indicating that these nanoparticles as the ideal materials for hosting guest molecules of various size, shapes, and functionalities. The corresponding pore size distribution (Figure 6) of MSNs calculated from the desorption branch of

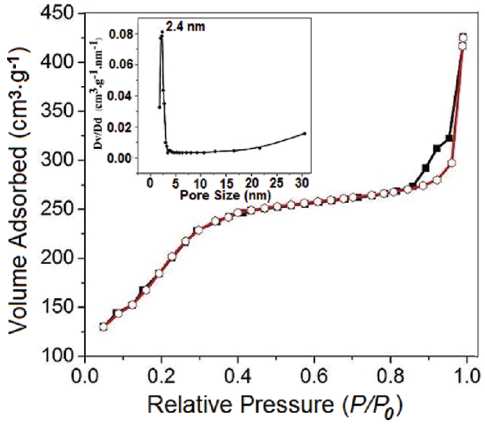

Figure 6. Nitrogen adsorption/desorption isotherms and pore size distribution of MSNs.

the nitrogen isotherms by using the Barrett–Joyner–Halenda (BJH) method had a narrow sharp peak at around 2.4 nm, which was consistent with the TEM result and suggested that a mesoporous reactive layer had been formed on the particle surface. Additionally, formation of these mesopores were highly favored as they had a high surface area and large pore, which allowed guest molecules to be hosted with them in the nanoscale porosity, thereby enhancing the capacity for drug adsorption.

3.2. Loading and Release of the Guest Molecules. To prove the redox-responsive gating behavior of the MSNs-SS-mPEG nanoparticles, we loaded fluorescein dye as a model drug, whose loading efficiency analyzed by UV–vis spectroscopy was about 8%, by soaking MSNs-SH nanoparticles in the phosphate-buffered saline (PBS) solution (pH 7.4) to evaluate the controlled release capacity of MSNs. The excessive fluorescein dye was removed by centrifugation and repeated washing with PBS solution. The resulting particles were then dispersed in the PBS buffer to test their controlled release property by UV–vis spectroscopy.

Release experiments were performed at different concentration of GSH. The relationship of released dye amount with the concentration of GSH was shown in Figure 7. It was noticed that little amounts of the dye released out into the solution under stirring 8 h in the absence of GSH, signifying efficient confinement of dye in the pores of the MSNs by virtue of capping with PEG chains. As the concentration of GSH increased, disulfide bonds were cleaved more quickly and the release of model drugs was effectively accelerated. Most importantly, the fast release of dye at the concentration of 10 mM GSH reached 43% at 1 h and 75% of the total dye at 22 h,

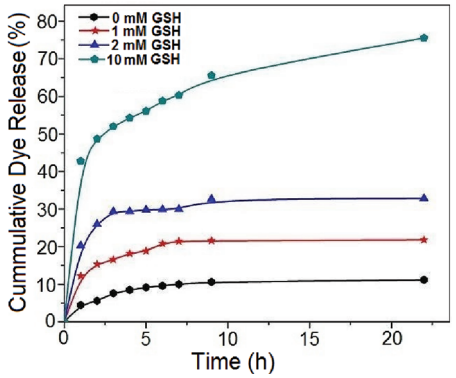

Figure 7. Cumulative release of fluorescein dye from MSNs-SS-mPEG nanoparticles.

which was consistent with cleavage of the PEG gatekeepers in the GSH solution. The above results suggested that the PEG chains as gatekeepers can retain the fluorescein molecules in the pores and still prevent undesired leaching from the mesopores in the absence of reduction environment, but the disulfide bond can be cleaved when under exposure to reduction condition (such as GSH, dithiothreitol (DTT), or mercaptoethanol (ME)) to induce the release of guest molecules.

Confocal laser scanning microscopy (CLSM) images of MCF-7 cells treated with dye-loaded MSNs-SS-mPEG nanoparticles further supported the suggestion that increasing the extracellular GSH concentrations could increase the induced-release amount of dye. Increasing extracellular GSH concentration can be expected to augment intracellular GSH concentration, then altering release kinetics of dye from MSNs-SS-mPEG nanoparticles.

Seen from Figure 8, green fluorescein dyes (as model drugs) were distributed in the cells, which indicated that most of dye-loaded MSNs-SS-mPEG nanoparticles were internalized into the endosome or lysosome after 24 h incubation. Furthermore, in contrast with the control, the green fluorescence signals of

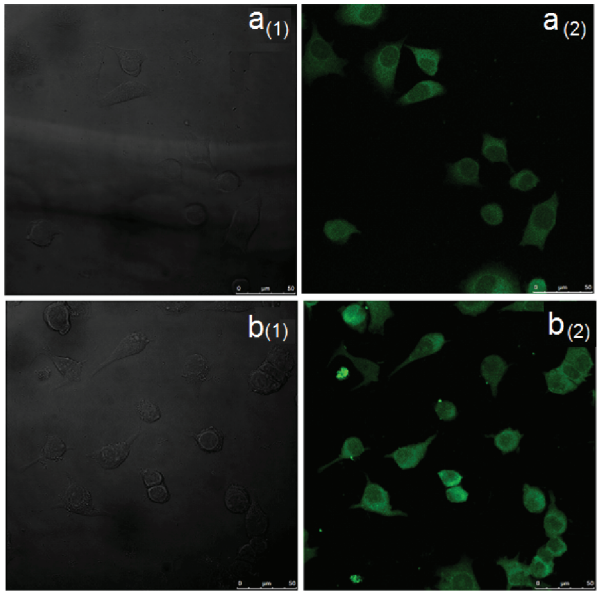

Figure 8. Representative CLSM images of dye-loaded MSNs-SS-mPEG nanoparticles incubated in MCF-7 cells for 6 h incubation, (a) no GSH, (b) 10 mM GSH.

dx.doi.org/10.1021/am3005225 | ACS Appl. Mater. Interfaces 2012, 4, 3177–3183

dye-loaded MSNs-SS-mPEG triggered by 10 mM GSH were obviously higher. This also suggested that PEG chains as gatekeepers were efficient to control release, which was consistent with the results of Figure 7.

3.3. Cytotoxicity. The cytotoxicity of MSNs-SS-mPEG nanoparticles should be investigated. Only nontoxic nanoparticles are suitable for drug delivery. In this work, the particle-induced cytotoxic effects on MCF-7 cells were evaluated using MTT.

The study on GSH-mediated drug release was carried out in MCF-7 cells in terms of GSH concentration and tumor cell viability. The intracellular GSH concentration[11] was controlled by using glutathione reduced ethyl ester (GSH-OEt) as an external enhancement of the cellular GSH level. GSH-OEt had no cytotoxicity and penetrated cellular membranes to generate GSH with rapid hydrolysis in cytoplasm. In Figure 9a, the

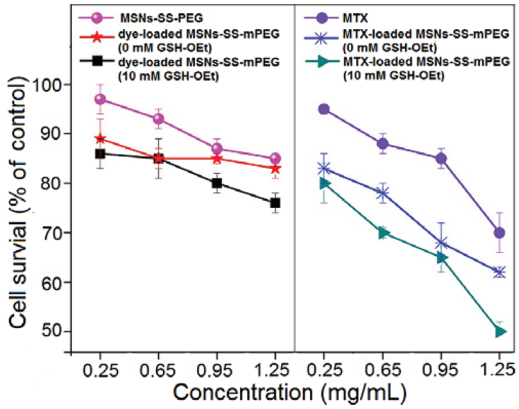

Figure 9. Cell survival of MCF-7 cells incubated with different concentrations of MSNs-SS-mPEG alone,dDye-loaded MSNs-SS-mPEG, MTX alone, and MTX-loaded MSNs-SS-mPEG nanoparticles after 24 h incubation.

results showed that cell viabilities of dye-loaded MSNs-SS-mPEG were ~85 and ~75% at the 0 and 10 mM GSH level at the concentration of 1.25 mg/mL, respectively, indicating that GSH can facilitate the release of the encapsulated guests at a controlled manner and the cell viability can also decrease with increasing the fluorescein dye amount. Although the carcinogenic effect of fluorescein dye has not been definitively identified, the benzene ring of fluorescein dye could affect the metabolism and DNA damage response pathways because of the situation that superoxide anion (O_2^-) generated by autoxidation of benzene metabolites may be the possible factor of benzene-induced cytotoxicity.[21,22] However, MSNs-SS-mPEG nanoparticles without dye did not significantly affect the cell proliferation even when the concentration was up to 1.25 mg mL^{-1}, suggesting that MSNs-SS-mPEG nanospheres have potential for drug loading and delivering into cancer cells. In Figure 9b, the MCF-7 cells were further incubated for 24 h with various concentrations of MTX-loaded MSNs-SS-mPEG (0.25, 0.65, 0.95, and 1.25 mg mL^{-1}). In the drug release study, MCF-7 cells in culture media were pretreated with 0 mM or 10 mM GSH-OEt for 22 h. The result also showed that GSH augmented the inhibitory effect of MTX-loaded MSNs-SS-mPEG, especially at the concentrations of 0.95 and 1.25 mg mL^{-1} for 24 h incubation due to the more cleavage of PEG shells induced by GSH-OEt. Compared with MTX-loaded MSNs-SS-mPEG, free MTX had the lower biological effect at the same concentration in Figure 9b. This was because drug resistance of MCF-7 could prevent the intracellular accumulation of the free MTX and cause a reduction in the cytotoxic activity. Besides, it was difficult to make MTX reach its main target and greatly compromise its biological effect due to the very poor solubility of MTX in water at neutral pH. Thus, MTX-loaded MSNs-SS-mPEG nanoparticles had the more noticeable biological effect at the same concentration.

4. CONCLUSIONS

In this work, disulfide-linked PEG chains were first chosen as gatekeepers to control release of guest molecules from pores of mesoporous silica nanoparticles (MSNs). Fluorescein dyes as model drug molecules were filled in the pores of MSNs and then blocked by adding mPEG-SS-Pyridine around the outer surface of mesoporous silica. The trapped molecules can be released from the mesopores due to addition of the reducing agent, such as GSH, resulting in disulfide cleavage. The higher the concentration of GSH is, the more the fluorescein dye molecules will be released from pores. In vitro cytotoxicity measured by MTT assay indicated that the MSNs-SS-mPEG nanoparticles had no cytotoxicity against MCF-7 cells. Additionally, the MTX-loaded MSNs-SS-mPEG nanoparticles has noticeable biological effect when the added concentration of MTX-loaded MSNs-SS-mPEG nanoparticles is more than 0.65 mg mL^{-1}. In all, the current gatekeepers with such unique properties are very promising for the development of smart molecular devices in drug delivery applications. However, further studies regarding controlling of larger-sized pores, optimization of MSNs-based system, and the delivery capabilities with various types of human cancer cells are now underway.

AUTHOR INFORMATION

Corresponding Author

*E-mail: wdpshk@tongji.edu.cn (D.W.); yongyong_li@tongji.edu.cn (Y.L.).

Notes

The authors declare no competing financial interest.

ACKNOWLEDGMENTS

This work was supported by Shanghai education commission innovative project (2011) and National Natural Science Foundation of China (21004045, 51173136 and 31100139).

REFERENCES

(1) (a) Liu, R.; Zhang, Y.; Zhao, X.; Agarwal, A.; Mueller, L. J.; Feng, P. Y. *J. Am. Chem. Soc.* **2010**, *132*, 1500−1501. (b) Gao, Q.; Xu, Y.; Wu, D.; Shen, W. L.; Deng, F. *Langmuir* **2010**, *26*, 17133−17140.

(2) (a) Schlossbauer, A.; Warncke, S.; Gramlich, P. M. E.; Kecht, J.; Manetto, A.; Carell, T.; Bein, T. *Angew. Chem., Int. Ed.* **2010**, *49*, 4734−4737. (b) Fu, Q.; Rao, G. V. R.; Ward, T. L.; Lu, Y. F.; Gabriel, P. L. *Langmuir* **2006**, *23*, 170−174.

(3) Coll, C.; Mondragón, L.; Martínez-Máñez, R.; Sancenón, F.; Dolores, M. M.; Soto, J.; Amorós, P.; Pérez-Payá, E. *Angew Chem. Int. Ed* **2011**, *50*, 2138−2140.

(4) (a) Lin, Q. N.; Huang, Q.; Li, C. Y.; Bao, C. Y.; Liu, Z. Z.; Li, F. Y.; Zhu, L. Y. *J. Am. Chem. Soc.* **2010**, *132*, 10645−10651. (b) Ferris, D.; Zhao, Y. -L.; Khashab, N. M.; Khatib, H. A.; Stoddart, J. F.; Zink, J. I. *J. Am. Chem. Soc.* **2009**, *131*, 1686−1688.

(5) (a) Kim, H.; Kim, S.; Park, C. Y.; Lee, H.; Park, H. J. *Adv. Mater.* **2010**, *22*, 4280−4283. (b) Liu, R.; Zhao, X.; Wu, T.; Feng, P. Y. *J. Am. Chem. Soc.* **2008**, *130*, 14418−14419.

(6) Lai, C. Y.; Trewyn, B. G.; Jeftinija, D. M.; Jeftinija, K.; Xu, S.; Jeftinija, S.; Lin, V. S. Y. *J. Am. Chem. Soc.* **2003**, *125*, 4451−4459.

(7) (a) Gan, Q.; Lu, X. Y.; Yuan, Y.; Qian, J. C.; Zhou, H. J.; Lu, X.; Shi, J. L.; Liu, C. S. *Biomaterials* **2011**, *32*, 1932−1942. (b) Giri, S.; Trewyn, B. G.; Stellmaker, M. P.; Lin, V. S.-Y. *Angew. Chem., Int. Ed* **2005**, *44*, 5038−5044.
(8) Muhammad, F.; Guo, M. Y.; Qi, W. X.; Sun, F. X.; Wang, A. F.; Guo, Y. J.; Zhu, G. S. *J. Am. Chem. Soc.* **2011**, *133*, 8778−8781.
(9) (a) Liu, R.; Zhang, Y.; Zhao, X.; Agarwal, A.; Mueller, L. J.; Feng, P. Y. *J. Am. Chem. Soc.* **2010**, *132*, 1500−1501. (b) Zhu, C. L.; Lu, C. H.; Song, X. Y.; Yang, H. H.; Wang, X. R. *J. Am. Chem. Soc.* **2011**, *133*, 1278−1281. (c) Vivero-Ecoto, J. L.; Slowing, I. I.; Wu, C. W.; Lin, V. S. Y. *J. Am. Chem. Soc.* **2009**, *131*, 3462−3463.
(10) Sun, J. T.; Hong, C. Y.; Pan, C. Y. *J. Phys. Chem. C* **2010**, *114*, 12481−12486.
(11) Koo, A. N.; Lee, H. J.; Kim, S. E.; Chang, J. H.; Park, C. Y.; Kim, C.; Park, J. H.; Lee, S. C. *Chem. Commun.* **2008**, *48*, 6570−6572.
(12) Wu, G. Y.; Fang, Y. Z.; Yang, Lupton, S. J. R.; Nancy, D. *J. Nutr.* **2004**, *134*, 489−492.
(13) Go, Y. M.; Jones, D. P. *Biochim. Biophys. Acta* **2008**, *1780*, 1273−1290.
(14) Mortera, R.; Vivero-Escoto, J.; Slowing, I. I.; Garrone, E.; Onida, B.; Lin, V. S. Y. *Chem. Commun.* **2009**, *22*, 3219−3221.
(15) Zhu, Y. F.; Fang, Y.; Borchardt, L.; Kaskel, S. *Microporous Mesoporous Mater.* **2011**, *141*, 199−206.
(16) Ferrari, M. *Curr. Opin. Chem. Biol.* **2005**, *9*, 343−346.
(17) Sun, H. L.; Guo, B. N.; Li, X. Q.; Cheng, R.; Meng, F. H.; Liu, H. Y.; Zhong, Z. Y. *Biomacromolecules* **2010**, *11*, 848−854.
(18) Cauda, V.; Argyo, C.; Bein, T. *J. Mater. Chem.* **2010**, *20*, 8693−8699.
(19) Wang, H. J.; Zhao, P. Q.; Liang, X. F.; Gong, X. Q.; Song, T.; Niu, R. F.; Chang, J. *Biomaterials* **2010**, *31*, 4129−4138.
(20) Fernandez, C. A.; Baumhover, N. J.; Duskey, J. T.; Khargharizi, S.; Kizzire, K.; Ericson, M. D.; Rice, K. G. *Gene Ther.* **2011**, *18*, 23−37.
(21) Atkinson, T. J. *Int. J. Hyg. Environ. Health* **2009**, *212*, 1−10.
(22) Ross, D. *Eur. J. Haematol.* **1996**, *57*, 111−118.